



Original Article

Novel biosynthesis of tellurium nanoparticles and investigation of their activity against common pathogenic bacteria



Nermine N. Abed, PhD^a, Inas M.M. Abou El-Enain, PhD^a,
Eman El-Husseiny Helal, PhD^b and Mohammed Yosri, PhD^{c,*}

^a Botany and Microbiology Department, Faculty of Science, Al-Azhar University, Nasr City, Cairo, Egypt

^b International Islamic Center for Population Studies and Research, Al-Azhar University, Cairo, Egypt

^c The Regional Center for Mycology and Biotechnology, Al-Azhar University, Nasr City, Cairo, Egypt

Received 12 July 2022; revised 17 September 2022; accepted 13 October 2022; Available online 29 October 2022

المخلص

أهداف البحث: يتحمل التيلوريوم اهتمام المعينين المتميزين لخصائصه الرائعة. تهدف هذه الدراسة لاختبار التأثير المضاد للبكتيريا في المختبر لجسيمات التيلوريوم النانوية المصنعة حيويًا من الشعيات ضد المكورات العنقودية المقاومة للميثاسيلين باعتبارها أحد مسببات الشائعة للأمراض البكتيرية في الدم. بالإضافة لذلك، تم اختبار تأثير جزيئات التيلوريوم النانوية ضد المكورات العنقودية المقاومة للميثاسيلين في الجسم الحي.

طريقة البحث: تم اختبار تسع عزلات من الشعيات لمعرفة قدرتها على تقليل تيلوريت البوتاسيوم إلى جزيئات التيلوريوم النانوية. تم التعرف على عزل الشعيات الأكثر كفاءة باستخدام البروتوكولات الجزيئية. تم تمييز التيلوريوم النانوية الناتجة عن طريق تطبيق أنواع مختلفة من الإشعاعات. تم الكشف عن الأنواع البكتيرية المسؤولة عن التهابات مجرى الدم في مستشفى الحسين. تم إجراء تحديد البكتيريا واختبار الحساسية للمضادات الحيوية باستخدام جهاز الفاينك 2. تم إجراء نماذج العدوى الحيوانية لاختبار فعالية التيلوريوم النانوية المنتجة مقابل المكورات العنقودية المقاومة للميثاسيلين المعزولة الأكثر شيوعًا باستخدام مقاييس البقاء، وعدد المستعمرات، وتقييم السيتوكينات، والاختبار الكيميائي الحيوي.

النتائج: تم التعرف على عزلة الشعيات الأكثر كفاءة على أنها المتسلسلة جرامميسولي وأعطيت رقم المنخل (أو إل 773539) كان متوسط حجم الجسيمات من الجسيمات النانوية المنتجة من التيلوريوم 21.4 نانومتر مع أشكال الأعداء والزهيرة. تم تحديد المكورات العنقودية المقاومة للميثاسيلين على أنها البكتيريا الرئيسية (60%) التي تسبب التهابات مجرى الدم، تليها الإشريكية القولونية (25%)، والكلبسيلا الرنوية (15%). تم اختبار جزيئات التيلوريوم

النانوية المنتجة مقابل المكورات العنقودية المقاومة للميثاسيلين باعتبارها البكتيريا الأكثر شيوعًا المعزولة من الدم والتي تظهر منطقة تثبيط عمل واعدة 0.7 ± 24 مم و التركيز التثبيطي الأدنى 50 ميكروغرام/مل. نموذج عدوى حيواني يعكس الإجراء الواعد لجزيئات التيلوريوم النانوية بمفردها أو بالاشتراك مع دواء معياري لمكافحة المكورات العنقودية المقاومة للميثاسيلين في نموذج العدوى الوريدي للفئران.

الاستنتاجات: يكون لجزيئات التيلوريوم النانوية جنبًا إلى جنب مع الفانكوميسين تأثير متتابع في مكافحة جراثيم الدم وتستحق مزيد من التحقق من النتائج.

الكلمات المفتاحية: المتسلسلة؛ جسيمات التيلوريوم النانوية؛ التهابات مجرى الدم؛ نشاط مضاد للجراثيم؛ المكورات العنقودية المقاومة للميثاسيلين

Abstract

Objectives: Tellurium has received substantial attention for its remarkable properties. This study performed *in vitro* and *in vivo* testing of the antibacterial action of tellurium nanoparticles biosynthesized in actinomycetes against methicillin-resistant *Staphylococcus aureus* (MRSA), a common blood bacterial pathogen.

Methods: Nine actinomycete isolates were tested for their potential to reduce potassium tellurite (K_2TeO_3) and form tellurium nanoparticles (TeNPs). The most efficient actinomycete isolate in producing Tellurium nanoparticles was identified through molecular protocols. The generated TeNPs were characterized using UV, TEM, EDX, XRD and FTIR. The bacterial species implicated in bloodstream infections were detected at El Hussein Hospital. Bacterial identification and antibiotic susceptibility testing were performed using Vitek 2. An animal infection model was used to test the efficacy of the produced TeNPs against the most commonly isolated methicillin-resistant *S. aureus* using

* Corresponding address: Dr. Mohammed Yosri, 11787, Nasr City, Cairo, Egypt.

E-mail: mohammed.yosri@yahoo.com (M. Yosri)

Peer review under responsibility of Taibah University.



Production and hosting by Elsevier

survival assays, colony counting, cytokine assessment and biochemical testing.

Results: The most efficient actinomycete isolate was identified as *Streptomyces graminisoli* and given the accession number (OL773539). The mean particle size of the produced TeNPs was 21.4 nm, and rods and rosette forms were observed. Methicillin-resistant *S. aureus* (MRSA) was the main bacterium (60%) causing blood stream infections, and was followed by *Escherichia coli* (25%) and *Klebsiella pneumoniae* (15%). The produced TeNPs were tested against MRSA, the bacterium most frequently isolated from blood, and showed a promising action inhibition zone of 24 ± 0.7 mm and an MIC of 50 $\mu\text{g/ml}$. An animal infection model indicated the promise of TeNPs alone or in combination with standard drugs to combat MRSA in a rat intravenous infection model.

Conclusion: TeNPs combined with vancomycin have successive impact to combat bacteremia for further verification of results.

Keywords: Antibacterial activity; Blood stream infections; MRSA; *Streptomyces* sp.; Tellurium nanoparticles

© 2022 The Authors. Published by Elsevier B.V. This is an open access article under the CC BY-NC-ND license (<http://creativecommons.org/licenses/by-nc-nd/4.0/>).

Introduction

Nanotechnology is an important approach with diverse impacts in various fields through the environmentally friendly synthesis of nanoscale particles (NPs) from plants and various micro-organisms.¹ Actinomycetes including *Streptomyces*, *Saccharopolyspora* and *Amycolatopsis* are unicellular microorganisms with high GC content that may have many beneficial applications.^{2,3} *Streptomyces* is the predominant actinomycete producing bioactive secondary metabolites with notable degrading activity.⁴ Many other studies have reported antimicrobial and anti-biofilm roles of compounds extracted from *Streptomyces*.⁵ Many drugs on the market are produced from *Streptomyces*.⁶

Tellurium (Te) is a natural rare metalloid on Earth with a notable toxicity to both prokaryotes and eukaryotes. It has a role in various industries including optics and electronics. It may be present as a harmful pollutant in the soil and water in areas near activity of these industries.^{7,8} Microorganisms such as *Rhodococcus erythropolis* have enzymes that reduce the toxicity of tellurite to zerovalent tellurium and can be used in bioremediation of regions contaminated with toxic tellurium.^{9,10} Nanoparticles have various features including a larger surface area and higher surface energy, and thus have roles in fields including biomedicine and pharmacology.^{11–14} Tellurium nanoparticles (TeNPs) have recently been used in research and industry, owing to their excellent biocompatibility,¹⁵ antimicrobial and antioxidant activity, ability to decrease cholesterol and triglyceride levels,¹⁶ and anticancer activity.^{17,18}

Bloodstream infections (BSI) have recently been reported to be caused by many resistant strains, thus leading to life-threatening effects.¹⁹ Primary BSI can be caused by microorganisms introduced directly into the bloodstream; for example, the use of contaminated medical devices can lead to primary infections. Secondary BSI is determined by the same organism causing infection in added mass tissue.²⁰ Vancomycin is commonly used to treat MRSA but often fails to eradicate this pathogen; therefore, alternative tools with effective action and minimal resistance must be explored through various methods.^{21–23}

In this study, TeNPs were synthesized by *Streptomyces graminisoli*. The produced NPs were characterized, and *in vitro* assessment of antibacterial activity against MRSA, the predominant pathogen in this study, was performed. *In vivo* determination of TeNP efficacy after intravenous injection of MRSA illustrated its potential pharmaceutical applications.

Materials and Methods

Sample collection and actinomycete isolation

Soil samples from various depths below the soil surface (from just beneath the surface to 1-foot depth) in Talkhaa-Daqhlia, Egypt, were collected in small sterile plastic bags. The soil samples were dried in a hot air oven at 60–65 °C to decrease the number of bacteria other than actinomycetes, according to Mahato et al.²⁴

Subsequently, 1 g of soil sample was transferred to 50 ml of sterile water, then placed in a rotary shaker at 120 rpm/min for 30 min. These solutions were serially diluted up to 10^{-10} , and 100 μl aliquots of the appropriate dilution were added to starch nitrate medium at pH 7.0 and incubated at 28 ± 2 °C for 7 days. Actinomycete colonies were selected on the basis of morphology and streaked on starch nitrate agar medium.²⁵ The isolates were stored in a refrigerator at 4 °C before further investigation.

Screening for TeNP-producing actinomycetes

All actinomycete isolates were grown on starch nitrate broth medium at 30 °C for 7 days under 150 rpm shaking conditions. The medium was filtered through a 0.45 μm pore size filter at the end of the incubation period to obtain a clear broth. Incubation at 30 °C for 48 h after the addition of the broth medium to 4 mmol of potassium tellurite (K_2TeO_3) was performed for each organism with 1 ml medium plus 2 mmol potassium tellurite solution. Tellurium oxide was indicated by the presence of black suspended particles, on the basis of comparison with blank samples. Actinomycete extracts and distilled water were used in equal volumes. The most promising TeNP producing isolate was selected according to the intensity of black particles.^{26–28}

Characterization of TeNPs

Various techniques were used to characterize the TeNPs. To determine the optical absorption of the TeNPs, we used a

UV–visible spectrophotometer (JENWAY 6305) operated at a resolution of 1 nm. The FTIR spectra of pellets were recorded using Fourier Transform Infrared spectroscopy (Bomen MB-154) to detect functional groups on NP surfaces. Transmission electron micrographs were taken with a Zeiss 902A TEM, operated at an acceleration voltage of 200 kV. Energy-dispersive X-ray analysis (EDX) demonstrated the presence of elemental tellurium. An X-ray micro-analyzer (Oxford 6587 INCA) attached to a JEOL JSM-5500 LV scanning electron microscope was used for EDX microanalysis at 20 kV. X-ray diffraction (XRD-6000) in a 2θ range from 10° to 130° was used to define the crystal shape.²⁹

Identification of selected isolates

The selected isolates producing TeNPs were identified according to their morphological, culture and physiological characteristics.^{30–34}

Actinomycetes were grown on starch agar slants for 7 days. Subsequently, 2 ml of spore suspension was inoculated into starch nitrate broth, and incubated on a shaking incubator for 3 days at 200 rpm and 30°C . Genetic material from cultured microorganisms was purified with a PCR product extraction kit (Qiagen, Valencia). DNA sequences were obtained with an Applied Biosystems 3130 genetic analyzer (HITACHI, Japan). Basic Local Alignment Search Tool (BLAST®) analysis was initially performed to establish sequence identity with respect to GenBank accessions. A phylogenetic tree was created with the MegAlign module in Lasergene DNA Star version 12.1. Phylogenetic analyses were performed with maximum likelihood, neighbor joining and maximum parsimony in MEGA6.^{35–37} Molecular analysis of the isolates was performed at the Biotechnology Unit, Reference Laboratory for Veterinary Quality Control on Poultry Production, Animal Health Research Institute, Dokki, Giza, Egypt.

Structural screening for isolated actinomycetes

For structural screening of *S. graminisoli*, cultures were prepared and investigated with scanning electron microscopy (JEOL, Japan) at the Regional Center for Mycology and Biotechnology, according to Abdulkhakimova et al.³⁸

Bacterial isolate collection and identification

A total of 100 blood samples were collected from patients admitted to the University Hospital El-Hussein between January 2020 and August 2021. The blood cultures were incubated aerobically at 37°C and observed daily for the first 3 days for the presence of visible microbial growth, according to hemolysis, gas production or coagulation of broth. Isolates were identified with standard microbiological techniques on the basis of Gram staining, colony characteristics and biochemical properties. The bacterial identification and antimicrobial susceptibility testing were performed using Vitec 2, including susceptibility testing and Staph AST-P620 card testing for MRSA (bioMérieux, France).^{39,24}

Antibacterial activity of TeNPs against methicillin resistant *S. aureus*

Mannitol salt agar was poured into Petri dishes and dried, and colonies of methicillin resistant *Staphylococcus aureus*

(MRSA) were streaked on the surface. In a well of 1 cm diameter in plates cultured with the MRSA, only 100 μl of TeNP suspension was added. An inhibition zone was observed after 24 h of incubation at 37°C .⁴⁰

Minimal inhibitory concentration determination of TeNPs

Müller-Hinton broth was enriched with TeNPs ranging from 0.062 mg/ml to 2 mg/ml, and inoculated with 5×10^5 colony forming units (CFU) of MRSA, then incubated at 37°C for 24 h. After incubation, 20 μl aliquots of 2,3,5-triphenyl-2H-tetrazolium chloride (TTC) solution (0.5 mg/ml) were added into the culture medium and shaken. After incubation for an additional 2 h at 37°C , the data were reported as MICs, and the lowest concentration of TeNPs showed no visible red color.⁴¹

Animal model

Female Wistar albino rats were purchased from the animal house of the Faculty of Medicine, Ain Shams University, and kept in sterile conditions for 14 days in an animal facility in the Regional Center for Mycology and Biotechnology. Sixty female Wistar albino rats weighing 170 g were divided into five groups ($n = 20$) as follows. The first group was a negative control group that was inoculated with deionized water. All other groups received intravenous injections of 100 μl of isolated and identified MRSA (10^5 CFU/ml as reported LD₅₀ dose with some modification)⁴² to induce bacteremia. The second group did not receive treatment. The third and fourth groups were injected intraperitoneally daily with 100 μl of vancomycin (Sigma) and 100 μl of TeNPs, respectively. The last group was inoculated with 100 μl of a combination of vancomycin and TeNPs (1:1). Animals were monitored daily, and killed through cervical dislocation at 3, 5 or 7 days for the experiments.

Survival assays

Rat survival rates were monitored daily for 2 weeks. At the end of experiment, mortality was verified, and a survival curve was drawn in GraphPad Prism version (5).⁴³

Determination of colony forming units

Bacterial counts in infected organs (lung, liver and kidneys) were conducted. Animals were killed by cervical dislocation at 3, 5 or 7 days. Organs were collected and digested in phosphate buffer. Homogenates were diluted and cultured on oxacillin resistance screening agar base medium for 24 h at 37°C , and the number of colonies in each group was recorded.⁴⁴

Cytokine assays

At day 7, blood was collected from sacrificed animal groups, and serum was separated. TNF- α , IL-1 β , IL-4 and IL-17 concentrations were measured according to the instructions of the commercial kits (Invitrogen, USA) used.²³

Blood function assays

Levels of aspartate aminotransferase (AST), gamma glutamyl transpeptidase (GGT) and blood urea nitrogen (BUN) were measured according to the instructions of the commercial kits (Thermo Fisher, USA) used.²³

Statistical analysis

Tests were performed three times, and the results are represented as mean \pm SEM. Statistical analysis was performed using (GraphPad Prism, version 5, USA). T-test and one-way analysis of variance were applied, and $P \leq 0.05$ was considered to indicate a statistically significant result.

Results

Culture, morphological, chemotaxonomic, physiological and biochemical characteristics of actinomycete isolates

The culture, morphological, chemotaxonomic, physiological and biochemical characteristics of the actinomycete isolates grown on different culture media are summarized in [Tables 1 and 2](#). The aerial hyphae of the isolate were gray, but the substrate mycelia were ivory, and light brown diffusible pigments formed on oatmeal agar. Melanin pigments formed on peptone yeast extract-iron agar. LL-diaminopimelic acid was detected in the whole hydrolysate of this strain, but no characteristic sugars were detected. Several factors such as carbon and nitrogen utilization, degradation tests, sensitivity tests, tolerance to NaCl, and growth pH and temperature were examined.

Sequencing of 16S rRNA genes and phylogenetic analysis

The 16S rRNA sequence was compared with the sequence of *Streptomyces* sp. to confirm the identification of the actinomycete isolate through multiple sequence alignment. Electrophoresis on agarose gels was used to analyze PCR amplification ([Supplement 1](#)). On the basis of multiple sequence alignment, this isolate showed 98.6% similarity to *S. graminisoli* ([Figure 1](#)). The sequence was submitted to the GenBank Nucleotide Sequence Database under accession number SUB10781525 *Streptomyces* OL773539 (<https://www.ncbi.nlm.nih.gov/nuccore/OL773539>).

Table 2: Chemotaxonomic, morphological and biochemical characteristics of the actinomycete isolates.

Characteristic	Result
Chemotaxonomic analysis:	
Cell wall hydrolysis for:	
Detection of diaminopimelic acid (DAP) isomers	LL-DAP
Sugar pattern	ND
Morphological characteristics:	
Spore chains	Spirals
Spore surface	Spiny
Spore mass color	Gray
Substrate mycelial color	Ivory
Diffusible pigment produced	–
Growth tests	
Range of pH: 4.0–10.0	+
Optimum temperature (°C): 25.0–45.0	+
Optimum salinity (%): 0.0–5.0	+
Biochemical characteristics:	
Nitrate reduction	+
Casein degradation	+
Urease production	–
Hydrogen sulfide production	–
Starch hydrolysis	+
Gelatin liquefaction	–
Methyl red test	+
Voges–Proskauer test	+
Cellulose degradation	+
Utilization of carbon source:	
Raffinose	+
Xylose	–
Glucose	+
Arabinose	+
Sucrose	+
Utilization of nitrogen source:	
L-Arginine	+
L-Asparagine	+
L-Cysteine-	–
L-Methionine -	–
L-Tryptophan-	–
L-Serine +	+
L-Valine+	+
L-Leucine-	–
L-Lysine-	–
Sensitivity assay:	
Penicillin G (10 i.u.)	+
Growth in the presence of sodium azide (0.01%, w/v)	+

(+) = positive, (–) = negative, (ND) = not detected.

Table 1: Cultural characteristics of the actinomycete isolates grown on different media.

Types of media	Growth	Substrate mycelium color	Aerial mycelium color	Diffusible pigments
Starch-nitrate agar	Good	Ivory	Gray	None
Inorganic-trace salt-starch agar	Good	Light yellow	Gray	None
Glycerol asparagine agar	Good	Ivory	Gray	None
Yeast extract-malt extract agar	Moderate	Ivory	Light gray	None
Oatmeal agar	Good	Ivory	Gray	Light brown
Melanin pigment media:				
1. Tryptone yeast extract broth	Weak	Ivory	Light gray	None
2. Peptone yeast extract iron agar	Moderate	Ivory	White	Light yellow
3. Tyrosine agar	Moderate	Ivory	White	None

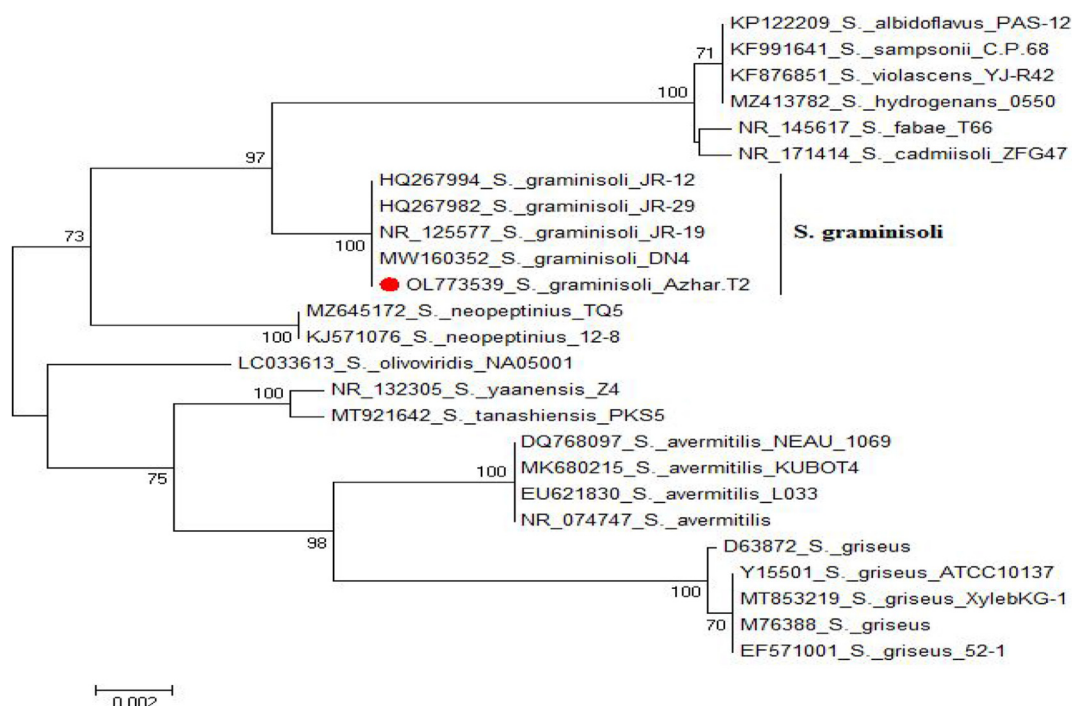


Figure 1: Phylogenetic analysis of *Streptomyces* isolates through neighbor joining.

Scanning electron microscopy

The electron micrographs and visual observations of the isolate indicated the morphological characteristics of the organism. The spore chain was composed of spiral spores with spiny surfaces (Figure 2).

Characterization of TeNPs

i. Visible analysis

The biosynthesis of TeNPs in the reaction tubes was identified by naked eye through black color formation (Figure 3A).

ii. UV–visible spectroscopy analysis

After inclusion of *S. graminisoli* extract in potassium tellurite solution, a UV scan from 200 to 800 nm was conducted. A broad peak of TeNPs was observed in this range, thus demonstrating the formation of TeNPs (Figure 3B).

iii. Energy dispersive X-ray analysis

EDX was performed to detect the presence and percentages of various elements potentially involved in the formation of TeNPs (Figure 3C). EDX analysis was conducted through detection of the power and magnitude of X-ray dissemination and indicated a tellurium percentage of 70.9% (Table 3).

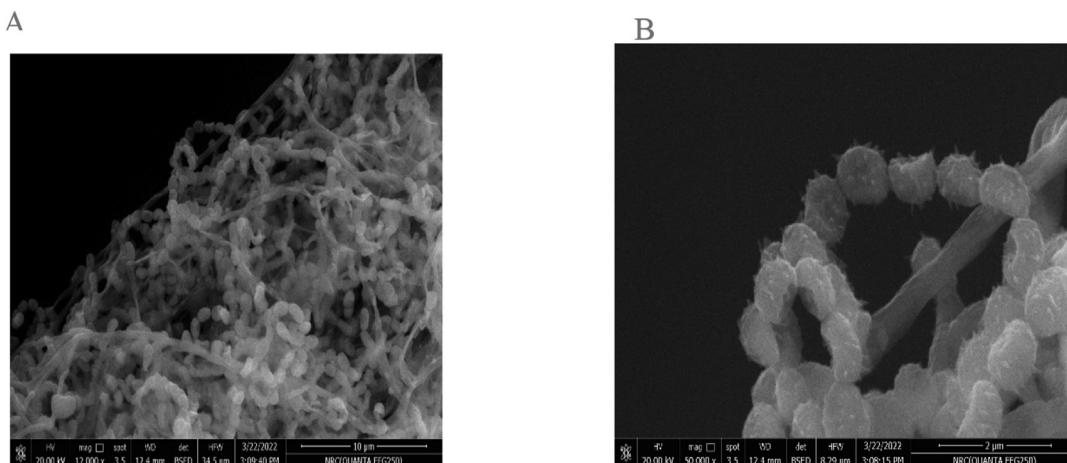


Figure 2: Scanning electron micrograph of *Streptomyces* isolate Azhar. T2. (A) 15,000 ×, (b) 50,000 ×.

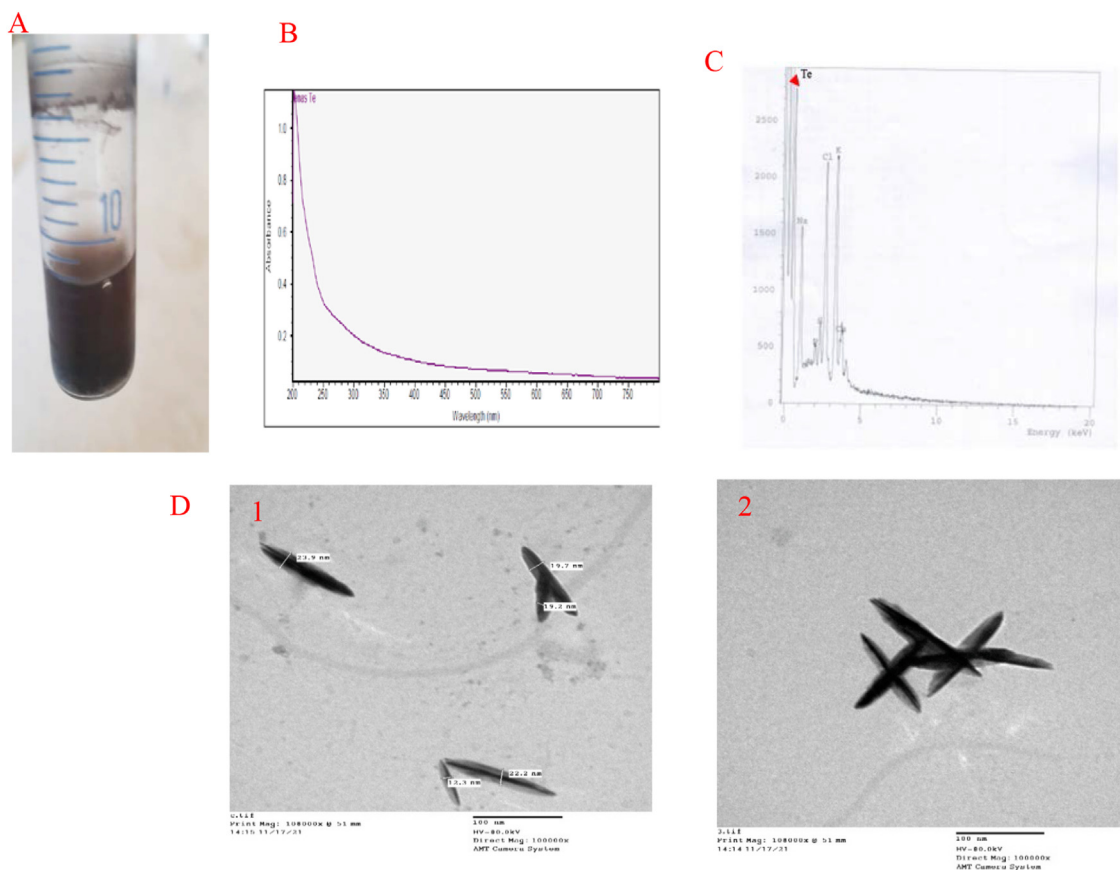


Figure 3: Characterization of tellurium nanoparticles (TeNPs): (A) Color produced in potassium tellurite solution after addition of *S. graminisoli* extract. (B) UV–visible spectra of TeNPs. (C) EDX spectrum of biosynthesized TeNPs. (D) TEM image of biosynthesized TeNPs at 10,000 × magnification: (1) rod shape; (2) rosette pattern.

iv. Microscopic characterization by TEM

Particles were measured after examination using transmission electron microscopy. The images represented various forms of NPs produced, including rods and rosette structures (Figure 3D). The mean size of the TeNPs was 21.4 nm (Table 1).

v. FTIR analysis

FTIR analysis was performed to detect the functional groups responsible for the activity of the TeNPs biosynthesized from actinomycete metabolites (Figure 4). The FTIR spectra of biosynthesized TeNPs showed different characteristic peaks at 446.68, 467.23, 522.93, 1643.51,

1642.83, 2083.73 and 3442.42 cm^{-1} . The strong broad peaks at 3442.42 and 1643.51 cm^{-1} may be associated with a primary amine or the amide N–H bond. The peak at 2083.73 cm^{-1} corresponded to C=C and O–H, whereas the peaks at 467.23 and 522.93 cm^{-1} were attributed to the formation of metal oxides. Thus, TeNPs might be due to various chemical groups in filtrate to reduce metal to metal oxide NPs.

vi. XRD analysis

XRD analysis (Figure 5) indicated the crystal structure of biosynthesized TeNPs. The 2θ peaks were at 23.4867 cm^{-1} , 27.707 cm^{-1} , 29.2989 cm^{-1} , 32.1699 cm^{-1} , 38.0074 cm^{-1} , 46.2036 cm^{-1} and 64.3965 cm^{-1} , corresponding to the

Table 3: Elemental percentage (%), determined with EDX and statistical measurements of TeNPs biosynthesized by *Streptomyces graminisoli*, imaged with TEM (mean ± SD).

EDX	Means of elements (%) ± standard deviation from mean (SD)					
Elements	Te	Cl	K	Na	P	S
%	70.9 ± 1.2	5.3 ± 0.3	6.7 ± 2.2	12.8 ± 0.63	2.39 ± 0.14	1.91 ± 0.11
TEM	Count	Mean	Minimum	Maximum		SD
TeNP size	25	21.4	18.81	24.0		5.03

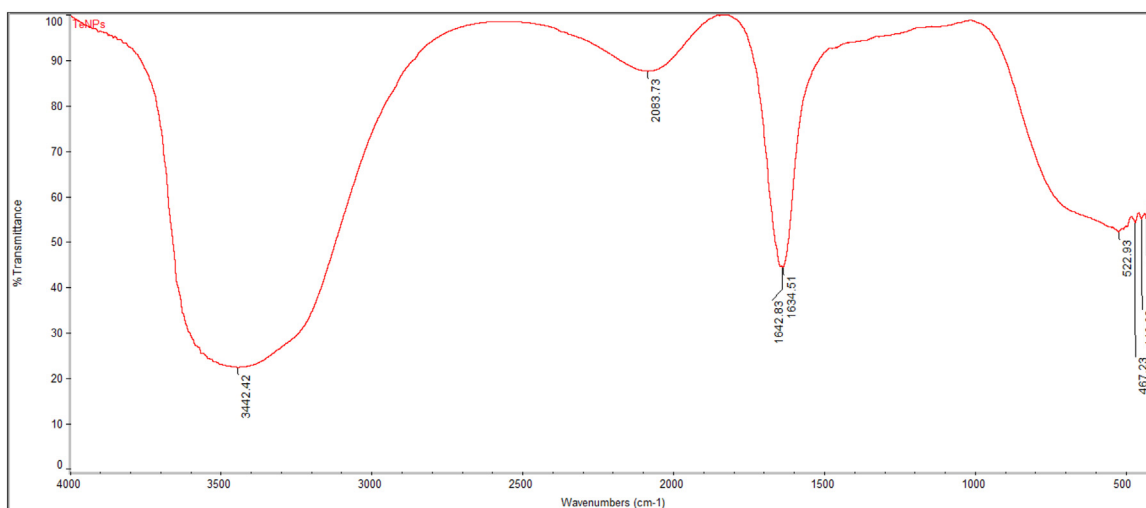


Figure 4: FT-IR spectrum of TeNPs produced by *Streptomyces graminisoli*.

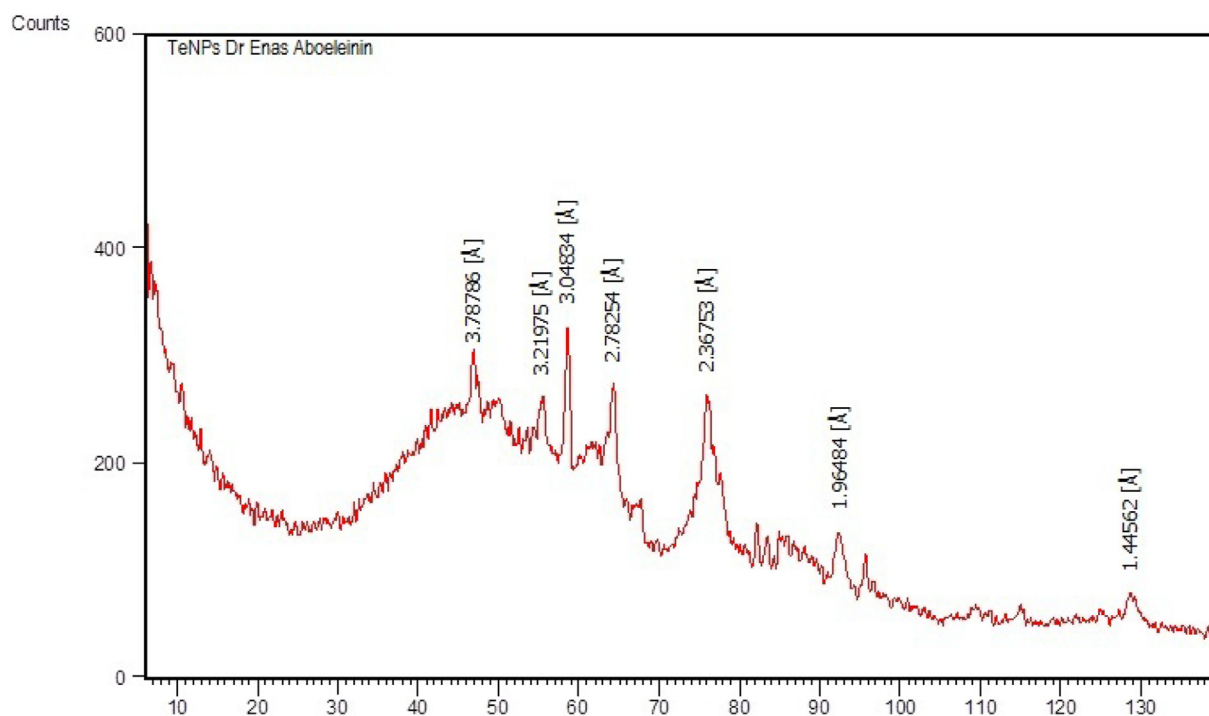


Figure 5: XRD pattern of TeNPs produced by *Streptomyces graminisoli*.

TeNPs synthesized. XRD analysis indicated impurity peaks, which may be caused by remnants of previous preparations and could be overcome using higher temperatures.

Identification of bacteria

A total of 100 blood cultures were collected from patients at the El Hussein Hospital and processed. Bacterial isolates were identified with a Vitec automated system; 60% of samples were identified as methicillin resistant *S. aureus*, while 25% of samples were *Escherichia coli*, and 15% of samples were *Klebsiella pneumoniae*. Therefore, MRSA was the most common bacterial isolate detected in this study (Supplement 2).

Antibacterial action and MICs of TeNPs against MRSA

TeNPs tested against the most common bacterial isolate in this study showed promising antibacterial action, with an

Table 4: In vitro anti-MRSA activity of biosynthesized tellurium NPs (TeNPs) and vancomycin, expressed as MIC ($\mu\text{g/ml}$) (mean \pm SD).

Treatments	Minimum inhibitory concentration ($\mu\text{g/ml}$)
TeNPs	50.13 \pm 0.26
Vancomycin	1.60 \pm 0.26

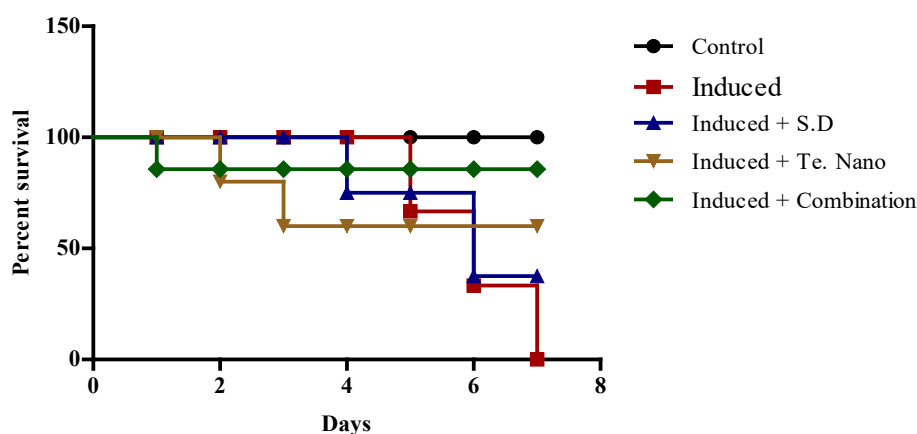


Figure 6: Survival rates of animals after intravenous injection with 1×10^5 CFU of MRSA. The survival rates of various groups are indicated: (1) control animals, (2) infected rats with no treatment, (3) infected animals treated with vancomycin as a standard drug, (4) infected animals treated with tellurium nanoparticles and (5) infected animals treated with a combination of standard drug and tellurium nanoparticles. The graph was drawn at the end of the experiment after 7 days.

inhibition zone of 24 ± 0.7 mm. The results of the serial dilution method, in which TTC reagent (tetrazolium test) was used to evaluate the MICs of the TeNPs against MRSA, showed that the minimum inhibitory concentration was 50 $\mu\text{g/ml}$. Thus, TeNPs had antibacterial action against MRSA and were further tested in an animal model (Table 4).

Survival assays

No difference was observed in survival in the first control group after 7 days. In the second group, infected animals showed weakness, and some gradually died during the experiment. In the third group of infected animals treated with a standard drug, 50% of animals died by the end of experiment. In the fourth group, the survival rate was approximately 70% among infected animals. Finally, infected animals treated with combination therapy showed a 90% survival rate (Figure 6).

CFU results

Lung, liver and kidney samples were processed and cultured after 3, 5 or 7 days in all groups, and the CFU count are shown in Tables 5–7. A significant decrease ($P \leq 0.05$) in bacterial count was observed in the tested organs of animals treated with the standard drug (vancomycin) or TeNPs. Administration of a combination of vancomycin and TeNPs markedly decreased ($P \leq 0.001$) the bacterial counts in the tested organs, thus showing very promising results.

Cytokine results

Serum levels of the inflammatory mediators TNF-alpha, IL1 β , IL-4 and IL-17 were measured after 7 days (Figure 7). A significant increase in TNF- α , IL-1 β and IL-17

Table 5: CFU counts in lungs in various groups of animals after 3, 5 or 7 days ($n = 3$). Data are presented as means \pm SD.

Time (days)	Control	Induced	Induced + SD	Induced + TeNP	Induced + combination
3	0	$4 \times 10^6 \pm 10$	$7 \times 10^4 \pm 9$	$5 \times 10^4 \pm 5$	$3 \times 10^2 \pm 3$
5	0	$5 \times 10^7 \pm 16$	$6 \times 10^3 \pm 14$	$3 \times 10^3 \pm 8$	$5 \times 10 \pm 2$
7	0	$7 \times 10^8 \pm 8$	$5 \times 10^2 \pm 13$	$2 \times 10^2 \pm 2$	$1 \times 10 \pm 1$

Table 6: CFU counts in livers in various groups of animals after 3, 5 or 7 days ($n = 3$). Data are presented as means \pm SD.

Time (days)	Control	Induced	Induced + SD	Induced + TeNP	Induced + combination
3	0	$1 \times 10^6 \pm 9$	$10 \times 10^4 \pm 11$	$4 \times 10^4 \pm 4$	$6 \times 10^2 \pm 4$
5	0	$2 \times 10^7 \pm 13$	$8 \times 10^3 \pm 7$	$3 \times 10^3 \pm 7$	$4 \times 10 \pm 3$
7	0	$5 \times 10^8 \pm 15$	$7 \times 10^2 \pm 3$	$2 \times 10^2 \pm 6$	$1 \times 10 \pm 1$

Table 7: CFU counts in kidneys in various groups of animals after 3, 5 or 7 days ($n = 3$). Data are presented as means \pm SD.

Time (days)	Control	Induced	Induced + S.D	Induced + TeNP	Induced + combination
3	0	$3 \times 10^6 \pm 16$	$6 \times 10^4 \pm 11$	6×10^4	$4 \times 10^2 \pm 5$
5	0	$4 \times 10^7 \pm 14$	$5 \times 10^3 \pm 7$	8×10^3	$2 \times 10 \pm 4$
7	0	$4 \times 10^8 \pm 13$	$5 \times 10^2 \pm 3$	3×10^2	$1 \times 10 \pm 10$

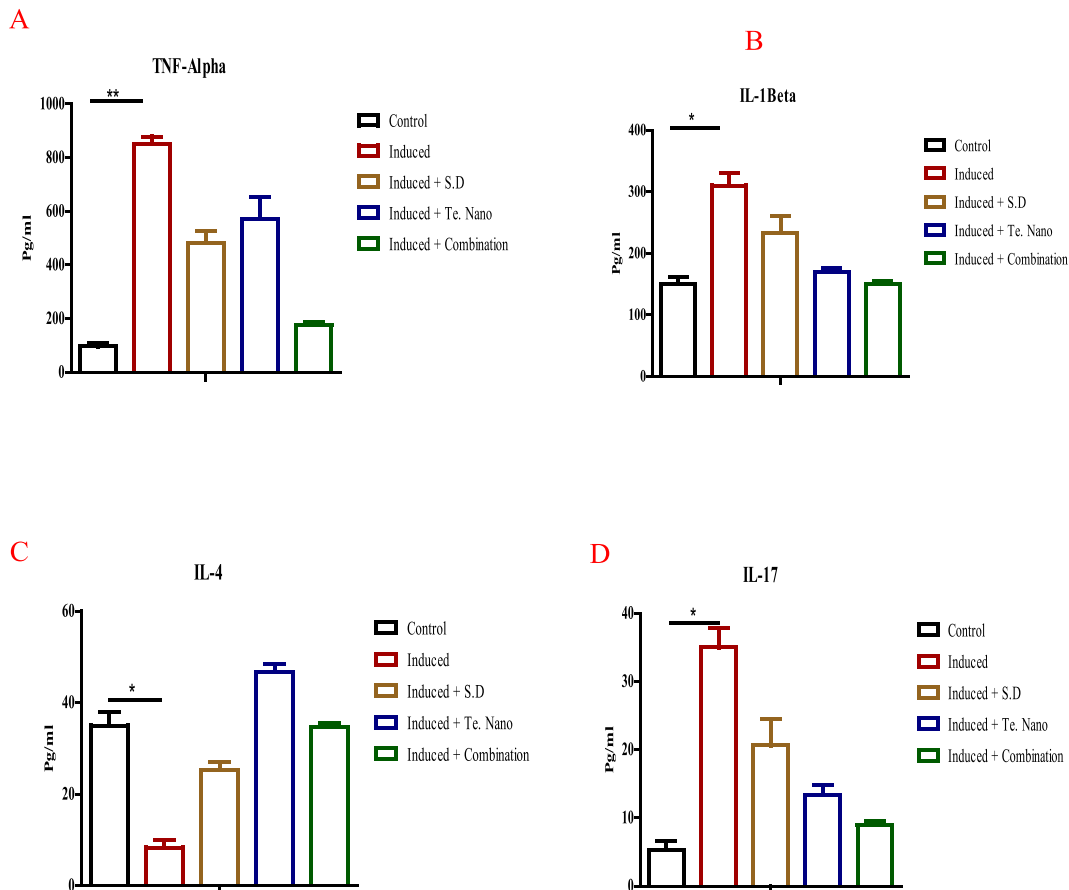


Figure 7: Cytokines in five groups: control; induced only; induced and treated with vancomycin; induced and treated with Te nanoparticles; and induced and treated with a combination of vancomycin and Te nanoparticles (n = 3). (A) TNF- α ; (B) IL-1 β ; (C) IL-4; and (D) IL-17. Data are presented as means \pm standard deviation; $P \leq 0.05$ is considered significant.

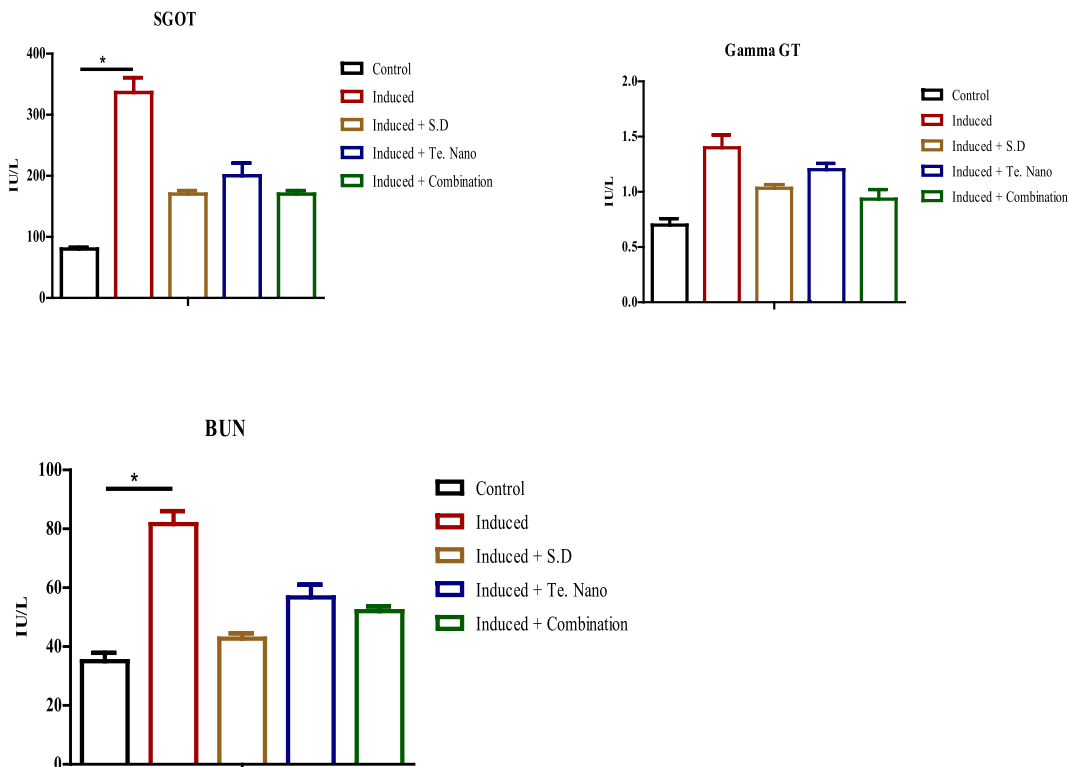


Figure 8: Liver and kidney function in five groups: control; induced only; induced and treated with vancomycin; induced and treated with Te nanoparticles; and induced and treated with a combination of vancomycin and Te nanoparticles (n = 3). (A) SGOT; (B) gamma GT; and (C) BUN. Data are presented as means \pm standard deviation. $P \leq 0.05$ is considered significant.

($P \leq 0.05$) was observed in the infected group, in contrast to the negative control group. Levels of the tested mediators significantly decreased ($P \leq 0.05$) with use of TeNPs, vancomycin and combination therapy, and combination therapy showed the best results relative to the negative control. Furthermore, IL-4 levels were significantly lower ($P \leq 0.05$) after induction of bacteremia in the second infected group than the negative control group. Combination therapy significantly increased IL-4 levels ($P \leq 0.05$) to values similar to those in uninfected animals.

Blood function results

Liver and kidney function was assessed on the basis of serum levels of SGOT, GGT and BUN in various groups of animals after 7 days (Figure 8). A significant increase ($P \leq 0.05$) in SGOT and BUN levels was observed after induction of bacteremia, in contrast to the negative control. However, the levels were lower ($P \leq 0.05$) in groups receiving vancomycin, TeNPs or combination therapy than in the second group. Furthermore, GGT levels were slightly higher after induction of bacteremia than those in the negative control and were slightly lower after the three treatments.

Discussion

Actinomycetes are a group of microorganisms isolated from various habitats including soil.⁴⁵ Actinomycetes contain diverse molecules and have vast biomedical applications, owing to their antimicrobial activity and immune-modulating activity.⁴⁶ In the present study, various actinomycetes were isolated from soil samples from Talkhaa-Daqhlia, Egypt, and nine isolates were obtained and stored for further testing.

Different microorganisms can be used to produce NPs through extra- or intracellular actions. These NPs have different applications and may be sensitive to various factors including light, heat and the level of the used element to biosynthesize nanoparticles.⁴⁷

TeNPs can be produced through many chemical methods, each with certain limitations. Consequently, researchers have tested green biosynthesis methods to prepare these types of NPs.⁴⁸ One method involves intracellular production by microorganisms and consequently requires additional steps to obtain pure TeNPs.²⁸

In the current study, actinomycete isolates were tested for biogenic formation of TeNPs in supernatant aliquots of nine isolates. Reduction of tellurium salt (K_2TeO_3) to tellurium metal (Te^0) indicated that this isolate had TeNP formation ability. Our findings were in accordance with those of Amoozegar et al.,²⁷ who screened 49 bacterial strains for the removal of tellurite and screened the filtrate using 200–800 nm range, and observed the ability of specific strains to reduce the tellurium salt.

In this study, one actinomycete isolate was identified to show the most promising TeNP production, and was subjected to morphological characterization, molecular identification and phylogenetic analysis. This isolate showed 98.6% similarity to *S. graminisoli*. Various research groups have used molecular techniques for the identification of

certain strains of actinomycetes producing natural beneficial products.^{49,50} Furthermore, examination of NPs through transmission electron microscopy indicated that the TeNP shapes comprised rod and rosette forms, with a mean particle size of 21.4 nm. Zare et al.⁵¹ have reported the same structure or TeNPs produced by bacteria.

EDX, FT-IR and FTIR analyses of the biosynthesized TeNPs reflected a tellurium percentage of 70.9%, and peaks corresponding to the functional groups and crystal structures reported by other research groups.^{52,53}

Emerging resistance to antibiotics has led researchers to investigate different types of resistant microorganisms, particularly blood borne types in hospitals, to overcome these life-threatening infections. In the present study, screening and identification of 100 blood culture samples of patients from a hospital in Cairo, Egypt, indicated the presence of many types of pathogenic bacteria, including MRSA, *E. coli* and *K. pneumoniae*. MRSA was the most common bacterial infection in this study, in line with findings from Licata et al.,⁵⁴ who screened confirmed blood stream infections in Italy and reported the presence of 12 invasive bacterial pathogens, among which oxacillin-resistant *S. aureus* were most common (28.1%). Furthermore, El-Sokkary et al.⁵⁵ have reported the predominance of multidrug-resistant bacteria as well as extensively drug-resistant bacteria (65.1% and 4.9%, respectively) in blood cultures of patients from various hospitals in low-, middle- and high-income countries.

Pugin et al.⁵⁶ have reported that TeNPs have no activity against MRSA strain 622-4, whereas Gupta et al.⁵⁷ have reported that TeNPs efficiently eradicate MRSA. Thus, the presence of various strains of hazardous pathogens indicates the need to apply various NPs to these isolated strains to overcome this problem, by alteration of the cell membrane⁵⁸ or production of reactive oxygen species.⁵⁹

In the current study, TeNPs enhanced the survival rates of infected animals, in line with findings from Cao et al.,⁶⁰ who have reported the efficiency of TeNPs in delivering cisplatin in tumor-induced animals with minimal adverse effects. Moreover, Gómez-Gómez et al.⁶¹ have confirmed the role of TeNPs in eradicating *E. coli* and *S. aureus* bacterial films, thus leading to changes in NP structure.

In the present study, TeNPs combined with standard drug treatment enhanced the protective effects against bacteremia, through decreasing bacterial counts in various crucial organs, upregulating the pro-inflammatory cytokines TNF- α and IL-1 β , downregulating the anti-inflammatory mediator IL-4 and regulating the concentration of (Th17) represented by IL-17. Our findings are in line with those from Hussain et al.,⁶² who have characterized the roles of NPs loaded with vancomycin in suppressing staphylococcal bacteremia and targeting infected organs to a greater extent than vancomycin alone. These effects may involve targeting of essential virulence factors of MRSA (e, g: β -toxin, FtsZ and Sortase B), which have essential roles in increasing the severity of MRSA infection in an induced model of bacteremia.⁶³

The synergistic effects of TeNPs with vancomycin in the current model enhanced activity against bacteremia with considerable safety with respect to liver and kidney function. Our findings are in line with those from Lee et al.,⁶⁴ who have tested the roles of NPs in targeting MRSA infections and the

filer small particle (20 nm) size by the kidney, thus leading to minimal burden with respect to blood function.

Conclusions

This study indicated that some isolated actinomycetes can be used for production of TeNPs with efficient activity against most common bacterial isolates from certain clinical settings, compared to the drug of choice. *In vivo* results revealed that TeNPs, either alone or combined with vancomycin, may provide a possible alternative to combat bacteremia in the future, after further verification.

Source of funding

This research did not receive any specific grant from funding agencies in the public, commercial, or not-for-profit sectors.

Conflict of interest

The authors have no conflict of interest to declare.

Ethical approval

The studies were approved by ethical committee of the Regional Center for Mycology and Biotechnology (No. RCMB2601202019).

Recommendations

S. graminisoli can produce TeNPs with antibacterial activity against certain blood bacterial infections and can be applied as a treatment against these infections after further confirmatory testing.

Author contributions

N.N.A., I.M.M.A. and E.E.H. conceived and designed the study. N.N.A., I.M.M.A., E.E.H. and M.Y. conducted research, provided research materials, and collected and organized data. M.Y. analyzed and interpreted data. M.Y. wrote the initial and final draft of article. All authors have critically reviewed and approved the final draft and are responsible for the content and similarity index of the manuscript.

Appendix A. Supplementary data

Supplementary data to this article can be found online at <https://doi.org/10.1016/j.jtumed.2022.10.006>.

References

- Ogunyemi SO, Zhang M, Abdallah Y, Ogunyemi SO, Zhang M, Abdallah Y, et al. The bio-synthesis of three metal oxide nanoparticles (ZnO, MnO₂, and MgO) and their antibacterial activity against the bacterial leaf blight pathogen. *Front Microbiol* 2020; 11:588326. <https://doi.org/10.3389/fmicb.2020.588326>.
- Behera BC, Sethi BK, Mishra RR, Dutta SK, Thatoi HN. Microbial cellulases – diversity & biotechnology with reference to mangrove environment: a review. *J Genetic Eng Biotechnol* 2017; 15: 197–210. <https://doi.org/10.1016/j.jgeb.2016.12.001>.
- Hozzein WN, Abuelsoud W, Wadaan MAM, Shuikan AM, Selim S, Jaouni SA, et al. Exploring the potential of actinomycetes in improving soil fertility and grain quality of economically important cereals. *Sci Total Environ* 2019; 651: 2787–2798. <https://doi.org/10.1016/j.scitotenv.2018.10.048>.
- Kadaikunnan S, Alharbi NS, Khaled JM, Alobaidi AS, Rajivgandhi GN, Ramachandran G, et al. Partially purified actinomycetes compounds enhance the intracellular damages in multi-drug resistant *P. aeruginosa* and *K. pneumoniae*. *Saudi J Biol Sci* 2021; 28(11): 6057–6062. <https://doi.org/10.1016/j.sjbs.2021.06.061>.
- Sun J, Shao J, Sun C, Song Y, Li Q, Lu L, et al. Cytotoxic and cell migration inhibiting agents from mangrove-derived Streptomyces rochei SCSIO ZJ89. *Bioorg Med Chem* 2018; 1;26(8): 1488–1494. <https://doi.org/10.1016/j.bmc.2018.01.010>.
- Jabila Mary TR, Kannan RR, Iniyam AM, Ramachandran D, Rakash PSG. Vincent Cell wall distraction and biofilm inhibition of marine Streptomyces derived angucycline in methicillin resistant *Staphylococcus aureus*. *Microb Pathog* 2021; 150: 104712. <https://doi.org/10.1016/j.micpath.2020.104712>.
- Di Tomaso G, Fedi S, Carnevali M, Manegatti M, Taddei C, Zannoni D. The membrane-bound respiratory chain of *Pseudomonas pseudoalcaligenes* KF707 cells grown in the presence or absence of potassium tellurite. *Microbiology* 2002; 148(Pt 6): 1699–1708. <https://doi.org/10.1099/00221287-148-6-1699>.
- Presentato A, Piacenza E, Darbandi A, Anikovskiy M, Cappelletti M, Zannoni D, et al. Assembly, growth and conductive properties of tellurium nanorods produced by *Rhodococcus aetherivorans* BCP1. *Sci Rep* 2018; 8(1): 3923. <https://doi.org/10.1038/s41598-018-22320-x>.
- Maltman C, Yurkov V. Extreme environments and high-level bacterial tellurite resistance. *Microorganisms* 2019; 22;7(12): 601. <https://doi.org/10.3390/microorganisms7120601>.
- Butz ZJ, Hendricks A, Borgognoni K, Ackerson CJ. Identification of a TeO₃- reductase/mycothione reductase from *Rhodococcus erythropolis* PR4. *FEMS Microbiol Ecol* 2020; 97(1): fiae220. <https://doi.org/10.1093/femsec/fiae220>.
- Chaudhary S, Umar A, Mehta SK. Selenium nanomaterials: an overview of recent developments in synthesis, properties and potential applications. *Prog Mater Sci* 2016; 83: 270–329. <https://doi.org/10.1016/j.pmatsci.2016.07.001>.
- Elahian F, Reisi S, Shahidi A, Mirzaei SA. High-throughput bioaccumulation, biotransformation, and production of silver and selenium nanoparticles using genetically engineered *Pichia pastoris*. *Nanomed Nanobiotechnol* 2017; 13: 853–861. <https://doi.org/10.1016/j.nano.2016.10.009>.
- Piacenza E, Presentato A, Zonaro E, Lampis S, Vallini G, Turner RJ. Selenium and tellurium nanomaterials. *Phys Sci Rev* 2018; 3. <https://doi.org/10.1515/psr-2017-0100>.
- Rasouli M. Biosynthesis of selenium nanoparticles using yeast *Nematospora coryli* and examination of their anti-candida and anti-oxidant activities. *IET Nanobiotechnol* 2019; 13: 214–218. <https://doi.org/10.1049/iet-nbt.2018.5187>.
- Medina Cruz D, Mi G, Webster TJ. Synthesis and characterization of biogenic selenium nanoparticles with antimicrobial properties made by *Staphylococcus aureus*, methicillin-resistant *Staphylococcus aureus* (MRSA), *Escherichia coli*, and *Pseudomonas aeruginosa*. *J Biomed Mater Res* 2018; 106: 1400–1412. <https://doi.org/10.1002/jbm.a.36347>.
- Mirjani R, Faramarzi MA, Sharifzadeh M, Setayesh N, Khoshayand MR, Shahverdi AR. Biosynthesis of tellurium nanoparticles by *Lactobacillus plantarum* and the effect of nanoparticle-enriched probiotics on the lipid profiles of mice.

- IET Nanobiotechnol 2015; 9: 300–305. <https://doi.org/10.1049/iet-nbt.2014.0057>.
17. Medina Cruz D, Tien-Street W, Zhang B, Huang X, Vernet Crua A, Nieto-Arguello A, et al. Citric juice-mediated synthesis of tellurium nanoparticles with antimicrobial and anticancer properties. *Green Chem* 2019; 21: 1982–1988. <https://doi.org/10.1039/c9gc00131j>.
 18. Vahidi H, Kobarfard F, Alizadeh A, Saravanan M, Barabadi H. Green nanotechnology-based tellurium nanoparticles: exploration of their antioxidant, antibacterial, antifungal and cytotoxic potentials against cancerous and normal cells compared to potassium tellurite. *Inorg Chem Commun* 2021; 124:108385. <https://doi.org/10.1016/j.inoche.2020.108385>.
 19. Eisenberg MA, Balamuth F. Pediatric sepsis screening in US hospitals. *Pediatr Res* 2022; 91(2):351358. <https://doi.org/10.1038/s41390-021-01708-y>.
 20. Santella B, Folliero V, Pirofalo GM, Serrettiello E, Zannella C, Moccia G, et al. Sepsis-A retrospective cohort study of blood-stream infections. *Antibiotics (Basel)* 2020; 9(12): 851. <https://doi.org/10.3390/antibiotics9120851>.
 21. Martin MA. Methicillin-resistant *Staphylococcus aureus*: the persistent nosocomial pathogen. *Curr Clin Top Infect Dis* 1994; 14: 170–191. <https://academic.oup.com/jac/article/41/3/325/680999>.
 22. Gardete S, Tomasz A. Mechanisms of vancomycin resistance in *Staphylococcus aureus*. *J Clin Invest* 2014; 124: 2836–2840. <https://doi.org/10.5772/67338>.
 23. Awad M, Yosri M, Abdel-Aziz MM, Younis AM, Sidkey NM. Assessment of the antibacterial potential of biosynthesized silver nanoparticles combined with vancomycin against methicillin-resistant *Staphylococcus aureus*—induced infection in rats. *Biol Trace Elem Res* 2021; 199: 4225–4236. <https://doi.org/10.1007/s12011-020-02561-6>.
 24. Mahato S, Lamichhane GC, Thakur A. Isolation and screening of antibiotic producing actinomycetes from soils of hills and plains of eastern Nepal. *J Clin Pharm* 2021; 5(1): 1019.
 25. Nandhini B, Josephine RM. A study on bacterial and fungal diversity in potted soil. *Int J Curr Microbiol App Sci* 2013; 2: 1–5.
 26. Taylor DE. Bacterial tellurite resistance. *Trends Microbiol* 1999; 7(3): 111–115. [https://doi.org/10.1016/s0966-842x\(99\)01454-7](https://doi.org/10.1016/s0966-842x(99)01454-7).
 27. Amoozegar MA, Ashengroph M, Malekzadeh F, Razavi MR, Naddaf S, Kabiri M. Isolation and initial characterization of the tellurite reducing moderately halophilic bacterium, *Salinococcus* sp. strain QW6. *Microbiol Res* 2008; 163: 456–465. <https://doi.org/10.1016/j.micres.2006.07.010>.
 28. Abo Elsouid MM, Al-Hagar OEA, Abdelkhalek ES, Sidkey NM. Synthesis and investigations on tellurium myconanoparticles. *Biotechnol Rep* 2018; 18:e00247. <https://doi.org/10.1016/j.btre.2018.e00247>.
 29. Krug P, Wiktorska K, Kaczyńska K, Ofiara K, Szterk A, Kuśmierz B, Mazur M. Sulfuraphane-assisted preparation of tellurium flower-like nanoparticles. *Nanotechnology* 2020; 31(5): 055603. <https://doi.org/10.1088/1361-6528/ab4e38>.
 30. Shirling EB, Gottlieb D. Methods for characterization of *Streptomyces* species. *Int J Syst Bacteriol* 1966; 16: 313–340. <https://doi.org/10.1099/00207713-16-3-313>.
 31. Shirling EB, Gottlieb D. Comparative descriptions of type culture of *Streptomyces* II. Species descriptions from the first study. *Int J Syst Bacteriol* 1968; 18: 69–189. <https://doi.org/10.1099/00207713-18-2-69>.
 32. Buchanan RE, Gibbson NE, editors. *Bergey's manual of determinative bacteriology*. 8th ed. Baltimore: Williams & Wilkins; 1974. <https://doi.org/10.1111/j.1550-7408.1975.tb00935.x>.
 33. Williams ST, Goodfellow M, Alderson G. Genus *Streptomyces*. In: Williams ST, Sharope ME, Holt JM, editors. *Bergey's manual of systematic bacteriology*. Baltimore: Williams & Wilkins; 1989. pp. 2452–2492.
 34. Hensyl WR. In: Holt JG, Williams ST, editors. *Bergey's manual of systematic bacteriology*. 9th ed. Baltimore: Williams & Wilkins; 1994.
 35. Altschul SF, Gish W, Miller W, Myers EW, Lipman DJ. Basic local alignment Search tool. *J Mol Biol* 1990; 215: 403–410. [https://doi.org/10.1016/S0022-2836\(05\)80360-2](https://doi.org/10.1016/S0022-2836(05)80360-2).
 36. Thompson JD, Higgins DG, Gibson TJ, Clustal W. Improving the sensitivity of progressive multiple sequence alignment through sequence weighting, position-specific gap penalties and weight matrix choice. *Nucleic Acids Res* 1994; 22(22): 4673–4680. <https://doi.org/10.1093/nar/22.22.4673>.
 37. Tamura K, Stecher G, Peterson D, Filipski A, Kumar S. MEGA6: molecular evolutionary genetics analysis version 6.0. *Mol Biol Evol* 2013; 30: 2725–2729. <https://doi.org/10.1093/molbev/mst197>.
 38. Abdulkhakimova D, Markhametova Z, Shamkeeva S, Zhulamanova A, Trenozhnikova L, Berezin V, et al. Characterization of extremophilic actinomycetes strains as sources of antimicrobial agents. *Methods Mol Biol* 2021; 2296: 59–75. https://doi.org/10.1007/978-1-0716-1358-0_4.
 39. Cartwright EJ, Paterson GK, Raven KE, Harrison EM, Gouliouris T, Kearns A, et al. Use of Vitek 2 antimicrobial susceptibility profile to identify mecC in methicillin-resistant *Staphylococcus aureus*. *J Clin Microbiol* 2013; 51(8): 2732–2734. <https://doi.org/10.1128/JCM.00847-13>.
 40. Kung JC, Wang WH, Lee CL, Hsieh HC, Shih CJ. Antibacterial activity of silver nanoparticles (AgNP) confined to meso-structured, silica-based calcium phosphate against methicillin-resistant *Staphylococcus aureus* (MRSA). *Nanomaterials* 2020; 10(7): 1264. <https://doi.org/10.3390/nano10071264>.
 41. Antachopoulos C, Meletiadiis J, Sein T, Roilides E, Walsh TJ. Concentration-dependent effects of caspofungin on the metabolic activity of *Aspergillus* species. *Antimicrob Agents Chemother* 2007; 51(3): 881–887. <https://doi.org/10.1128/AAC.01160-06>.
 42. Van den Berg S, Laman JD, Boon L, ten Kate MT, de Knegt GJ, Verdijk RM, et al. Distinctive cytokines as biomarkers predicting fatal outcome of severe *Staphylococcus aureus* bacteremia in mice. *PLoS One* 2013; 8(3):e59107. <https://doi.org/10.1371/journal.pone.0059107>.
 43. Yimin KM, Zhao S, Ozaki M, Haga S, Nan G, et al. Contribution of toll-like receptor 2 to the innate response against *Staphylococcus aureus* infection in mice. *PLoS One* 2013; 8(9): e74287. <https://doi.org/10.1371/journal.pone.0074287>.
 44. Shatzkes K, Singleton E, Tang C, Zuena M, Shukla S, Gupta S, et al. Predatory bacteria attenuate *Klebsiella pneumoniae* burden in rat lungs. *mBio* 2016; 7(6): e01847. <https://doi.org/10.1128/mBio.01847-16>. e01816.
 45. Bhatti AA, Haq S, Bhat RA. Actinomycetes benefaction role in soil and plant health. *Microb Pathog* 2017; 111: 458–467. <https://doi.org/10.1016/j.micpath.2017.09.036>.
 46. Wibowo JT, Kellermann MY, Köck M, Putra MY, Murniasih T, Mohr KI, et al. Anti-infective and antiviral activity of valinomycin and its analogues from a sea cucumber-associated bacterium, *Streptomyces* Sp. SV 21. *Mar Drugs* 2021; 19: 81. <https://doi.org/10.3390/md19020081>.
 47. Koul B, Poonia AK, Yadav D, Jin JO. Microbe-Mediated biosynthesis of nanoparticles: applications and future prospects. *Biomolecules* 2021; 11(6): 886. <https://doi.org/10.3390/biom11060886>.
 48. Zonaro E, Lampis S, Turner RJ, Qazi SJS, Vallini G. Biogenic selenium and tellurium nanoparticles synthesized by environmental microbial isolates efficaciously inhibit bacterial planktonic cultures and biofilms. *Front Microbiol* 2015; 6: 584. <https://doi.org/10.3389/fmicb.2015.00584>.
 49. Siegl T, Luzhetskyy A. Actinomycetes genome engineering approaches. *Antonie Leeuwenhoek* 2012; 102(3): 503–516. <https://doi.org/10.1007/s10482-012-9795-y>.

50. Wang C, Lu Y, Cao S. Antimicrobial compounds from marine actinomycetes. **Arch Pharm Res (Seoul)** 2020; 43(7): 677–704. <https://doi.org/10.1007/s12272-020-01251-0>.
51. Zare B, Faramarzi MA, Sephezadeh Z, Shakibaie M, Rezaie S, Shahverdi AR. Biosynthesis and recovery of rod-shaped tellurium nanoparticles and their bactericidal activities. **Mater Res Bull** 2012; 47: 3719–3725. <https://doi.org/10.1016/j.materresbull.2012.06.034>.
52. Najimi S, Shakibaie M, Jafari E, Ameri A, Rahimi N, Forootanfar H, et al. Acute and subacute toxicities of biogenic tellurium nanorods in mice. **Regul Toxicol Pharmacol** 2017; 222–230. <https://doi.org/10.1016/j.yrtph.2017.09.014>.
53. Medina Cruz D, Tien-Street W, Zhang B, Huang X, Vernet Crua A, Nieto-Argüello A, et al. Citric juice-mediated synthesis of tellurium nanoparticles with antimicrobial and anticancer properties. **Green Chem** 2019; 21(8): 1982–1988. <https://doi.org/10.1039/c9gc00131j>.
54. Licata F, Quirino A, Pepe D, Matera G, Bianco A. Collaborative group. Antimicrobial resistance in pathogens isolated from blood cultures: a two-year multicenter hospital surveillance study in Italy. **Antibiotics (Basel)** 2020; 10(1): 10. <https://doi.org/10.3390/antibiotics10010010>.
55. El-Sokkary R, Uysal S, Erdem H, et al. Profiles of multidrug-resistant organisms among patients with bacteremia in intensive care units: an international ID-IRI survey. **Eur J Clin Microbiol Infect Dis** 2021; 40: 2323–2334. <https://doi.org/10.1007/s10096-021-04288-1>.
56. Pugin B, Cornejo FA, García JA, Díaz-Vásquez WA, Arenas FA, Vásquez CC. Thiol-mediated reduction of *Staphylococcus aureus* tellurite resistance. **Adv Microbiol** 2014; 4: 183–190. <https://doi.org/10.4236/aim.2014.44024>.
57. Gupta PK, Sharma PP, Sharma A, Khan ZH, Solank PR. Electrochemical and antimicrobial activity of tellurium oxide nanoparticles Mater. **Sci. Eng. B** 2016; 211: 166–172. <https://doi.org/10.1016/j.mseb.2016.07.002>.
58. Pi J, Yang F, Jin H, Huang X, Liu R, Yang P, et al. Selenium nanoparticles induced membrane bio-mechanical property changes in MCF-7 cells by disturbing membrane molecules and F-actin. **Bioorg Med Chem Lett** 2013; 23: 6296–6303. <https://doi.org/10.1016/j.bmcl.2013.09.078>.
59. Zhang Y, Hu M, Zhang W, Zhang X. Construction of tellurium-doped mesoporous bioactive glass nanoparticles for bone cancer therapy by promoting ROS-mediated apoptosis and antibacterial activity. **J Colloid Interface Sci** 2022; 610: 719–730. <https://doi.org/10.1016/j.jcis.2021.11.122>.
60. Cao W, Li F, Ruofan C, Xu H. Tellurium-containing nanoparticles for controlled delivery of cisplatin based on coordination interaction. **RSC Adv** 2016; 6: 94033–94037.
61. Gómez-Gómez B, Sanz-Landaluce J, Teresa Pérez-Corona M, Madrid Y. Fate and effect of in-house synthesized tellurium based nanoparticles on bacterial biofilm biomass and architecture. Challenges for nanoparticles characterization in living systems. **Sci Total Environ** 2020; 719:137501. <https://doi.org/10.1016/j.scitotenv.2020.137501>.
62. Hussain S, Joo J, Kang J, Kim B, Braun GB, She ZG, et al. Antibiotic-loaded nanoparticles targeted to the site of infection enhance antibacterial efficacy. **Nat Biomed Eng** 2018; 2(2): 95–103. <https://doi.org/10.1038/s41551-017-0187-5>.
63. Mohammed LJ, Chehri K, Karimi I, Karimi N. Computational insight into the protective mechanism of *Allium iranicum* Wendelbo. Alliaceae in a mouse model of Staphylococcosis: focus on dietary phytocannabinoid *trans*-caryophyllene. **Silico Pharmacol** 2021; 9(1): 17. <https://doi.org/10.1007/s40203-021-00078-x>.
64. Lee NY, Ko WC, Hsueh PR. Nanoparticles in the treatment of infections caused by multidrug-resistant organisms. **Front Pharmacol** 2019; 10: 1153. <https://doi.org/10.3389/fphar.2019.01153>.

How to cite this article: Abed NN, Abou El-Enain IMM, El-Husseiny Helal E, Yosri M. Novel biosynthesis of tellurium nanoparticles and investigation of their activity against common pathogenic bacteria. *J Taibah Univ Med Sc* 2023;18(2):400–412.